RESEARCH ARTICLE

The Expression of MRTF-A and AQP1 Play Important Roles in the Pathological Vascular Remodeling

Yong Jiang*

Abstract

Background: Objective Myocardin-related transcription factor (MRTF)-A is a Rho signaling-responsive co-activator of serum response factor (SRF). The purpose of this study is to investigate the role of MRTF-A and AQP1 (aquaporin 1) in pathological vascular remodeling. Materials and Methods: MRTF-A, AQP1 and neointima expression was detected both in the wire injured femoral arteries of wild-type mice and the atherosclerotic aortic tissues of ApoE$^{-/-}$ mice. Expression of ICAM-1, matrix metallopeptidase 9 (MMP-9) and integrin β1 were also assayed. The intercourse relationship between the molecules were investigated by interfering RNA and inhibitor assay. Results: MRTF-A and AQP1 expression were significantly higher in the wire injured femoral arteries of wild-type mice and in the atherosclerotic aortic tissues of ApoE$^{-/-}$ mice than in healthy control tissues. Both in wire-injured femoral arteries in MRTF-A knockout (Mkl1$^{-/-}$) mice and atherosclerotic lesions in Mkl1$^{-/-}$; ApoE$^{-/-}$ mice, neointima formation were significantly attenuated and the expression of AQP1 were significantly decreased. Expression of ICAM-1, matrix metallopeptidase 9 (MMP-9) and integrin β1, three SRF targets and key regulators of cell migration, and AQP1 in injured arteries was significantly weaker in Mkl1$^{-/-}$ mice than in wild-type mice. In cultured vascular smooth muscle cells (VSMCs), knocking down MRTF-A reduced expression of these genes and significantly impaired cell migration. Underlying the increased MRTF-A expression in dedifferentiated VSMCs were the down-regulation of microRNA-300. Moreover, the MRTF-A inhibitor CCG1423 significantly reduced neointima formation following wire injury in mice. Conclusions: MRTF-A could be a novel therapeutic target for the treatment of vascular diseases.

Keywords: Myocardin-related transcription factor (MRTF)-A - aquaporin 1 (AQP1)

Asian Pac J Cancer Prev, **16 (4)**, 1375-1383

Introduction

Myocardin-related transcription factor (MRTF)-A (Mkl1, Bsac or Mal) and MRTF-B (Mkl2) are transcriptional cofactors that associate with serum response factor (SRF) (Franco et al., 2013; Weinl et al., 2014), an MADS box transcription factor and critical modulator of cardiovascular differentiation and growth, promoting transcription of a subset of genes involved in cytoskeletal organization and muscle differentiation (Ni et al., 2013; Wang et al., 2013; Weinl et al., 2013). AQP1 plays an important role in the differentiation and maintenance of cardiac and smooth muscle cell lineage and angiogenic endothelial cells formation. AQP1, which is related to angiogenesis and migration of endothelial cells, can strongly express in tumor microvascular endothelia and its deletion can reduce breast tumor growth and lung metastasis in tumor-producing MMTV-PyVT mice (Esteva-Font et al., 2014) . By contrast, MRTF-A and MRTF-B are expressed more ubiquitously and are found in both the cytoplasm and nucleus (Minami et al., 2012). In serum-starved fibroblasts, MRTF-A and MRTF-B are localized mainly in the cytoplasm and are translocated into the nucleus in response to stimulation with serum or other stimuli that promote Rho family GTPase activation and subsequent actin polymerization (Minami et al., 2012; Wang et al., 2012). Thus, MRTF-A and MRTF-B transduce Rho family GTPase-actin signaling from the cytoplasm to SRF in the nucleus (Shen et al., 2011). Correspondingly, MRTF-A can promote the migration of MCF-7 breast cancer cells (Zhang et al., 2013).

Aquaporins (AQPs) are a family of small integral membrane proteins related to the major intrinsic protein. This gene encodes an aquaporin which functions as a molecular water channel protein. It is a homotetramer with 6 bilayer spanning domains and N-glycosylation sites. Several transcript variants encoding different isoforms have been found for this gene. AQPs play key roles in tumor biology. And the expression of these proteins is altered in mammary tumors and in breast cancer cell lines (Mobasheri et al., 2014). In contrast to AQP1, the roles played by MRTF-A in VSMC differentiation and phenotypic modulation remain unclear, though a recent human genetic analysis detected an association between coronary artery disease (CAD) and a single-nucleotide polymorphism (SNP) in the promoter region

*Laboratory Medical College, Jilin Medical College, Jilin, P.R.China *For correspondence: jiangyongpost@sina.com*

of the MRTF-A gene that enhances the gene expression (Jin et al., 2010) reported that MRTF-A knockout mice were born in anticipated Mendelian ratios, whereas some studies reported that MRTF-A knockout mice were born at less than the anticipated Mendelian ratio, which they attributed to fetal loss due to heart failure (Nakamura et al., 2010). In both groups, however, live born MRTF-A knockout pups showed no obvious gross abnormality or cardiovascular defect under normal conditions, except for a defect in maternal lactation due to impaired phenotypic modulation of mammary gland myoepithelial cells (Jeon et al., 2010). Other studies indicated that MRTF-A might be an important regulator of mammary gland and can be involved in cancer metastasis and that Histone methyltransferase SMYD3 can promote MRTF-A-mediated transactivation of MYL9 and migration of MCF-7 breast cancer cells (Luo et al., 2014) .

In the present study, we investigated the potential roles of MRTF-A in the pathological processes underlying vascular proliferative diseases and the possible mechanisms involved in it. The purpose of our study is to provide experimental evidence for clinical target therapy of vascular diseases.

Materials and Methods

Plasmids

-930 bp MRTF-A(-184C)-luc (MRTF-A-luc), ICAM-1-luc, ICAM-1 CArG-mut-luc and 3×CArG-luc were described previously (Weinl et al., 2013). Expression vectors used in the experiments were described previously (Ni et al., 2013). MRTF-A 3'UTR-luc and mut MRTF-A 3'UTR-luc were respectively generated by inserting the MRTF-A 3'UTR containing wild type or mutated miR-300 target sequences downstream of the luciferase gene in a pMIR-REPORTER kit miRNA reporter expression vector (Ambion). -5500 bp MRTF-A-luc was generated by inserting 5500 bp of the 5'-FR of MRTF-A gene upstream of the luciferase gene in pGL4 vector (Promega).

Animal experiments

MRTF-A$^{-/-}$ mice were kindly provided from Dr EN Olson (The University of Texas, Southwestern Medical Center at Dallas). ApoE$^{-/-}$ and MRTF-A$^{-/-}$ mice (C57BL/6 background) were cross-bred. The animal care and all experimental protocols were reviewed and approved by the Animal Research Committee at Jilin Medical College.

Cell culture and transfection

RAVSMCs (Cell Applications. Inc.), A7r5 (DS Pharma Biomedical), NIH3T3 and COS7 cells were maintained in DMEM supplemented with 10% FCS. Co-transfection of RAVSMCs with 3×CArG-luc plus expression plasmids encoding MRTF-A (1 ng) and STARS (100 ng), or with MRTF-A-luc plus expression plasmids encoding AQP1 and MRTF-A (0, 1 or 10 ng each) was accomplished using FuGene6 (Roche). pRL-TK (Roche) was included in all transfections as an internal control. MiRIDIAN microRNA mimic for miR-300, miRIDIAN microRNA hairpin inhibitor for miR-300 or a negative control for each (Thermo Scientific) was transfected into RAVSMCs grown in 6-cm dishes using Dharmafect2. MAVSMCs were obtained as previously reported (Shen et al., 2011).

Mouse vascular injury

Vascular wire injury was induced in femoral arteries of male C57BL/6 wild-type or Mkl1$^{-/-}$ mice at 8-10 weeks of age, as described previously (Davis-Dusenbery et al., 2011). LNA oligonucleotide anti-miR-300 microRNA inhibitor or LNA microRNA inhibitor negative control (20 mg/kg) (50-FAM prelabelled, Exiqon) was injected into sham-operated or injured femoral arteries from the muscular branch using a syringe with 29 gauge needle (TERUMO).

Quantification of neointimal hyperplasia

We harvested the femoral and carotid arteries 4 weeks after wire injury, unless otherwise indicated. Digitalized images were analysed using image analysis software (Image J, NIH), and the intimal and medial areas were recorded. The average of the neointima/media ratios in FIVE serial sections was designated as the value to represent each individual.

Wound healing experiments

The cells (5×10^5) were seeded in 6-well plates and after 24 h, when the cells had grown by 90-100%, they were scraped with a pipette tip to generate straight wounds. To ensure documentation of the same region, the wells were marked across the wounded area. The medium was replaced with a serum free medium (RPMI-1640, Wisent Inc., St-Bruno, QC, Canada) and the cells were treated with a medium containing 1 mM mitomycin to inhibit cell division. Phase contrast images were recorded under an inverted microscope (Nikon ECLIPSE Ti-E, Nikon, Kobe, Japan) at the time of wounding, 0 h, and at 24 h. The untreated cells served as controls.

Analysis of atherosclerotic lesion area in ApoE$^{-/-}$ mice

Mkl1$^{+/+}$; ApoE$^{-/-}$ and Mkl1A$^{-/-}$; ApoE$^{-/-}$ mice were fed normal chow for 4 weeks beginning when the mice were 4 weeks old. Then beginning when they were 8 weeks old, they were fed a high cholesterol diet (F2HFD1, Oriental Biotechnology) for 8 weeks. Atherosclerotic lesions were analysed by en-face analysis of the whole aorta and quantified by cross-sectional analysis of the proximal aorta.

PCR

RNA isolation and reverse transcription were performed as previously described (Wang et al., 2012). Oligonucleotide primer sequences were as follows: β-actin (264bp), forward: 5'-GAG ACC TTC AAC ACC CCA GCC-3'; reverse: 5'-AAT GTC AC G CAC GATT TCC C-3'; MRTF-A (201bp), forward: 5'-TCC CCA TCG CCA TCC CC-3' reverse: 5'-CAC CAT GGC CTC GGC TGG-3'. For all the above genes, amplification was performed under the same cycling conditions (1 minute at 94°C, 50 seconds at 57°C, 1 minute at 72°C), except the number of cycles that were specified for each gene (32 for MRTF-A).

Western blot and Immunoprecipitation

Cells were harvested at specific times after treatment

with regents as indicated in each experiment. Cells were mixed with loading buffer and subject to electrophoresis. After electrophoresis, proteins were transferred to polyvinyl difluoride membranes (Pall Filtron) using a semidry blotting apparatus (Pharmacia) and probed with mouse mAbs, followed by incubation with peroxidase-labeled secondary antibodies. Detection was performed by the use of a chemiluminescence system (Amersham) according to the manufacturer's instructions. Then membrane was striped with elution buffer and reprobed with antibodies against the nonphosphorylated protein as a measure of loading control. Controls for the immnoprecipitation used the same procedure, except agarose beads contained only mouse IgG.

Luciferase assay

Forty-eight hours after transfection, the cells were rinsed in PBS. Experiments for each treatment were performed in triplicate. Luciferase activity was assessed using the dual-luciferase reporter assay system (Promega, WS, USA) with a luminometer (Promega, WS, USA). The luciferase activity after cell lysis was measured and then normalized to the activity of renilla luciferase driven by the constitutional promoter in the phRL vector. Basal promoter activity was measured relative to the activity observed with the pGL3 vector alone.

RNA-i experiments

The si-RNA sequence targeting human MMP-9 (from mRNA sequence; Invitrogen online) corresponds to the coding region 377-403 relative to the first nucleotide of the start codon (target=5'-AAC ATC ACC TAT TGG ATC CAA ACT AC-3'). Computer analysis using the software developed by Ambion Inc. confirmed this sequence to be a good target. si-RNAs were 21 nucleotides long with symmetric 2-nucleotide 3'overhangs composed of 2'-deoxythymidine to enhance nuclease resistance. The si-RNAs were synthesized chemically and high pressure liquid chromatography purified (Genset, Paris, France). Sense si-RNA sequence was 5'-CAU CAC CUA UUG GAU CCA AdT dT-3'. Antisense si-RNA was 5'-UUG GAU CCA AUA GGU GAU GdT dT-3'. For annealing of si-RNAs, mixture of complementary single stranded RNAs (at equimolar concentration) was incubated in annealing buffer (20 mM Tris-HCl pH 7.5, 50 mM NaCl, and 10 mM $MgCl_2$) for 2 minutes at 95°C followed by a slow cooling to room temperature (at least 25°C) and then proceeded to storage temperature of 4°C. Before transfection, cells cultured at 50% confluence in 6-well plates (10 cm^2) were washed two times with OPTIMEM 1 (Invitrogen) without FCS and incubated in 1.5 ml of this medium without FCS for 1 hour. Then, cells were transfected with MMP-9-RNA duplex formulated into Mirus TransIT-TKO transfection reagent (Mirus Corp, Interchim, France) according to the manufacturer's instructions. Unless otherwise described, transfection used 20 nM RNA duplex in 0.5 ml of transfection medium OPTIMEM 1 without FCS per 5×10^5 cells for 6 hours and then the medium volume was adjusted to 1.5 ml per well with RPMI 2% FCS. SilencerTM negative control 1 si-RNA (Ambion Inc.) was used as negative control under similar conditions (20 nM).The efficiency of silencing is 80% in our assay.

Statistical analysis

Results are expressed as mean±standard deviation. Data were analysed using the unpaired two-tailed student's t test and the log rank test. P values of $p<0.05$ were considered significant.

Results

Increased expression of MRTF-A in femoral arteries after wire injury

To explore the potential role played by MRTF-A during pathological vascular remodelling, we initially compared the expression of AQP1, MRTF-A and MRTF-B mRNA between femoral arteries subjected to wire injury or to a sham operation. As seen previously (Du et al., 2009), levels of AQP1 mRNA were significantly up-regulated in

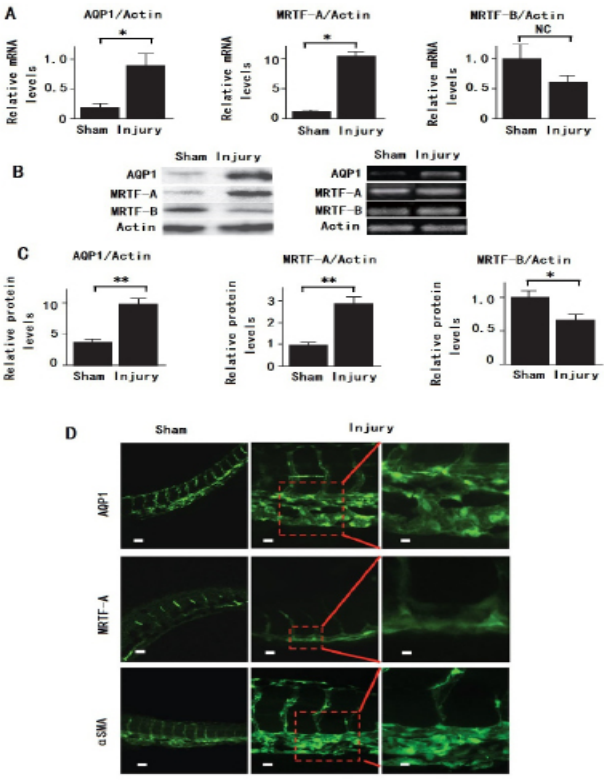

Figure 1. Increased Expression of MRTF-A in Femoral Arteries after Wire Injury in Mice. (A) Real-time RT–PCR analysis showing relative levels of AQP1, MRTF-A and MRTF-B mRNAs (normalized to Actin mRNA) in femoral arteries 2 weeks after wire injury (injury) (n=6 each). The relative mRNA level in sham-operated arteries (sham) was assigned a value of 1.0. (B) Representative western blots and PCR showing AQP1, MRTF-A and MRTF-B in wire-injured and sham-operated femoral arteries (2 weeks after injury). (C) The relative protein levels (normalized to Actin) of AQP1, MRTF-A and MRTF-B in wire-injured and sham-operated femoral arteries (n=4 each). The relative protein level in the sham-operated arteries was assigned a value of 1.0. (D) Immunohistochemical analysis of MRTF-A expression in sham-operated and wire injured femoral arteries. Tissues are labelled with anti-BSAC (MRTF-A) or anti-α-smooth muscle actin (α SMA) antibodies; bar indicates 100 μm. Three different experiments gave identical results. All graphs are shown as means±s.e.m. *$p<0.05$. **$p<0.001$. NC, not significant

femoral arteries 2 weeks after wire injury, while levels of MRTF-B mRNA were not significantly affected (Figure 1A). By contrast, expression of MRTF-A mRNA was significantly increased in injured arteries, as compared to sham-operated arteries (Figure 1A). Western blot and PCR analysis using specific antibodies for AQP1, MRTF-A and MRTFB, respectively, clearly showed that the level of AQP1 protein was increased in injured arteries, whereas MRTF-A protein was significantly increased (Figure 1B and C). Immunohistochemical analysis showed that cells positively stained for MRTF-A were located mainly in the neointima of injured arteries (Figure 1D). Moreover, in serial sections stained for α-smooth muscle actin (αSMA), most of the cells that positively stained for MRTF-A also positively stained for αSMA (Figure 1D).

Attenuated vascular remodelling after wire injury in MRTF-A knockout mice

To further evaluate the function of MRTF-A during vascular remodeling, next we performed wire injury in the femoral arteries of MRTF-A knockout ($Mkl1^{-/-}$) mice. As previously reported (Hanna et al., 2009), the $Mkl1^{-/-}$ mice were viable, fertile and showed no significant gross abnormalities or cardiovascular defects under normal conditions. There was no difference in blood pressure or heart rate between wild-type and $Mkl1^{-/-}$ mice (Figure 2A). Femoral arterial expression of AQP1 mRNA was significantly higher in $Mkl1^{-/-}$ mice 2 weeks after wire injury than in sham-operated arteries, just as was observed with wild-type mice (Figure 2B). On the other hand, neointima-to-medial ratios determined 4 weeks after wire injury were significantly smaller in $Mkl1^{-/-}$ mice than in wild-type mice (Figure 2C). Four weeks after wire injury, the neointimal area comprised cells positively stained for αSMA was markedly smaller in $Mkl1^{-/-}$ mice than in wild-type mice (Figure 2D). Immunohistochemical analysis in serial sections stained for SM-MHC showed overlap with αSMA-positive cells, suggesting that a reduction in the

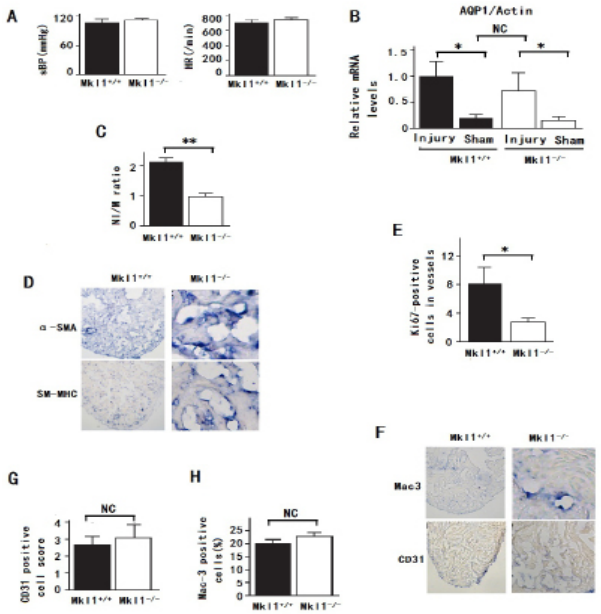

Figure 2. Attenuated Vascular Remodelling in Response to Wire Injury in $Mkl1^{-/-}$ Mice. (A) Systolic blood pressure (sBP) and heart rate (HR) in control $Mkl1^{+/+}$ and $Mkl1^{-/-}$ mice (n=5 each). (B) The relative levels of AQP1 mRNA in wire-injured and sham-operated femoral arteries in $Mkl1^{+/+}$ and $Mkl1^{-/-}$ mice (n=5 each). (C) The neointima (NI)-to-media (M) ratio in arteries 4 weeks after wire injury in $Mkl1^{+/+}$ and $Mkl1^{-/-}$ mice (n=20 each). (D) Representative images of neointima in arteries 4 weeks after wire injury in Mkl1+/+ and $Mkl1^{-/-}$ mice. α-SMA: staining with anti-α-SMA antibody. SM-MHC: staining with anti-SM-MHC antibody. (E) Numbers of Ki-67-positive cells in injured vessels of $Mkl1^{+/+}$ and $Mkl1^{-/-}$ mice 4 weeks after wire injury are shown (n=3 in each group). (F) Representative images of neointima stained with anti-CD31 (CD31) or anti-Mac3 (Mac3) antibody in arteries from $Mkl1^{+/+}$ and $Mkl1^{-/-}$ mice 4 weeks after wire injury. (G, H) The semi-quantitative CD31-positive scores (n=5 in each group) (G) and the relative numbers of Mac3-positive cells (% positive cells/total cells in neointima and media; n=4 in each group) (H) in $Mkl1^{+/+}$ and $Mkl1^{-/-}$ mice 4 weeks after wire injury are shown. All graphs are shown as means±s.e.m. *p<0.05. **p<0.001. NC, not significant

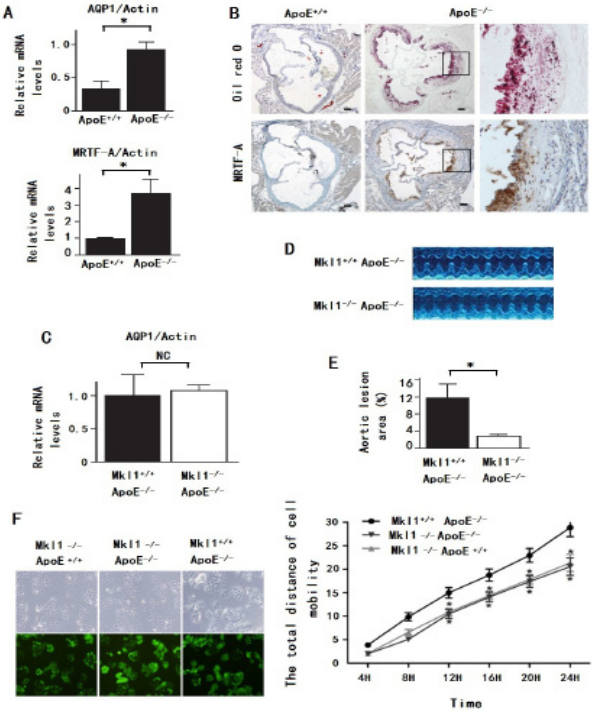

Figure 3. Atherosclerotic lesions in $Mkl1^{-/-}$; $ApoE^{-/-}$ mice are attenuated, as compared to those in $Mkl1^{+/+}$; $ApoE^{-/-}$ Mice. (A) Real-time RT-PCR analysis showing the relative levels of MRTF-A and AQP1 mRNAs (normalized to Actin mRNA) in atherosclerotic aortas from $ApoE^{-/-}$ mice fed a high-cholesterol diet and normal aortas from $ApoE^{+/+}$ mice at 16 weeks of age (n=4 each). *p<0.05. (B) Representative images showing MRTF-A expression within an atherosclerotic lesion in the proximal aorta of $ApoE^{-/-}$ mice. The tissues from $ApoE^{+/+}$ and $ApoE^{-/-}$ mice were stained using anti-BSAC antibodies (MRTF-A). Three different experiments gave identical results. (C) Real-time RT-PCR analysis showing the relative levels of AQP1 mRNA in atherosclerotic aortas from $Mkl1^{-/-}$; $ApoE^{-/-}$ and $Mkl1^{+/+}$; $ApoE^{-/-}$ mice fed a high-cholesterol diet (n=4 each). (D) Representative images of atherosclerotic lesions from an en-face analysis of the total aorta in $Mkl1^{+/+}$; $ApoE^{-/-}$ and $Mkl1^{-/-}$; $ApoE^{-/-}$ mice fed a high-cholesterol diet. Three independent experiments showed identical results. (E) Graphs showing the relative (%) area of atherosclerotic lesions in cross-sections of proximal aorta from $Mkl1^{+/+}$; $ApoE^{-/-}$ and $Mkl1^{-/-}$; $ApoE^{-/-}$ mice fed a high cholesterol diet for 8 weeks (n=8 each). (F) The moving ability at the aortic root of $Mkl1^{-/-}$; $ApoE^{-/-}$ mice and $Mkl1^{+/+}$; $ApoE^{-/-}$ mice. *p<0.05. SM-MHC: staining with anti-SM-MHC antibody. Bar indicates 100 μm. All graphs are shown as means±s.e.m

numbers of dedifferentiated VSMCs within the neointima is largely responsible for the reduction in the neointima-to-medial ratios seen in Mkl1$^{-/-}$ mice (Figure 2D). Indeed, the numbers of Ki-67-positive proliferating cells within the injured vessels were also significantly lower in Mkl1$^{-/-}$ mice than in wild-type mice (Figure 2E). In addition, because multiple cell types other than dedifferentiated VSMCs can contribute to neointima formation and to the vascular remodeling process, we also stained the tissue for endothelial cell (CD31) and macrophage (Mac3) markers. The relative numbers of CD31-positive and Mac3-positive cells in the injured arteries did not differ between wild-type and Mkl1$^{-/-}$ mice (Figure 2F), which indicates that a reduction in the number of αSMA-positive dedifferentiated VSMCs contributes to the attenuation of vascular remodeling in wire-injured Mkl1$^{-/-}$ mice. It showed no significant difference in the semi-quantitative CD31-positive scores and the relative numbers of Mac3-positive cells between Mkl1$^{+/+}$ and Mkl1$^{-/-}$ mice 4 weeks after wire injury (Figure 2G and 2H) .

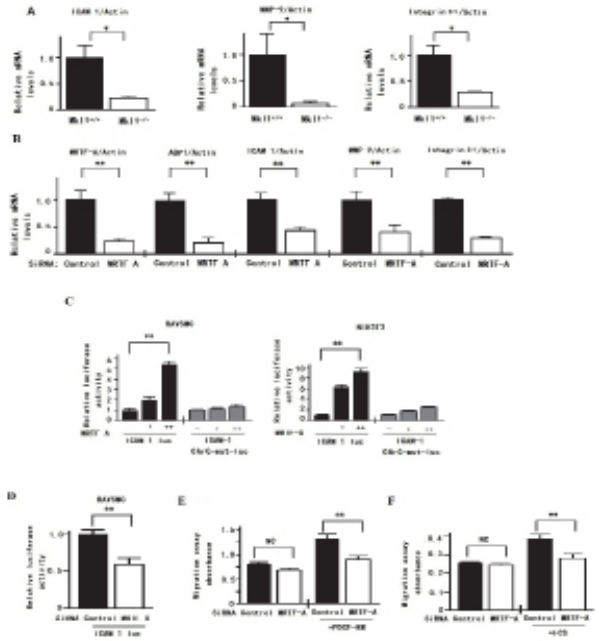

Figure 4. MRTF-A mediatesAcquisition of Migration capacity by Dedifferentiated VSMCs Through Regulation of SRF-Target Genes. (A) Real-time RT-PCR analysis showing relative levels of ICAM-1, MMP9 and integrin β1 mRNAs (normalized to Actin mRNA) in femoral arteries 2 weeks after wire injury in Mkl1$^{+/+}$ and Mkl1$^{-/-}$ mice (n=4 each). (B) Real-time RT–PCR analysis showing relative levels of MRTF-A, AQP1, ICAM-1, MMP9 and integrin β1 mRNAs in RAVSMCs transfected with MRTF-A siRNA or control siRNA (n=6 each). (C) Co-transfection of a plasmid expressing MRTF-A (0, 10 and 100 ng) plus the luciferase reporter gene driven by bp -360 to +63 of the 5'-flanking region of ICAM-1 gene (ICAM-1-luc) into RAVSMCs (left panel) and NIH3T3 cells (right panel). Relative luciferase activities normalized to Renilla luciferase (pRL-TK) activity are shown. ICAM-1 CArG-mut-luc: luciferase reporter gene driven by the ICAM-1 promoter harbouring a mutation within the CArG-box. Data were obtained from three experiments performed in sex tuplicate. (D) Co-transfection of MRTF-A siRNA plus vinculin-luc into RAVSMCs. Relative luciferase activities normalized to Renilla luciferase activity are shown. Data were obtained from two experiments performed in sex tuplicate. (E) Migration in the presence or absence of PDGF-BB of RAVSMCs transfected with MRTF-A siRNA or control siRNA. Data were obtained from three experiments performed in sex tuplicate. (F) Migration in the presence or absence of fetal calf serum (FCS) of RAVSMCs transfected with MRTF-A siRNA or control siRNA. Data were obtained from three experiments performed in sex tuplicate. All graphs are shown as means±s.e.m. *p<0.05. **p<0.01. NC, not significant

Loss of MRTF-A attenuates atherosclerotic lesions in APOE$^{-/-}$ mice

We next sought to analyse MRTF-A expression in a model of a different type of vascular disorder. ApoE$^{-/-}$ mice are prone to atherosclerotic lesions, to which both dedifferentiated VSMCs and infiltrating inflammatory cells contribute. MRTF-A gene expression was significantly up-regulated in aortic tissues containing atherosclerotic lesions in ApoE$^{-/-}$ mice fed a high cholesterol diet for 8 weeks (from 8 to 16 weeks of age), as compared to normal wild-type aortic tissues in age-matched mice (Figure 3A). By contrast, AQP1 gene and MRTF-A gene expression

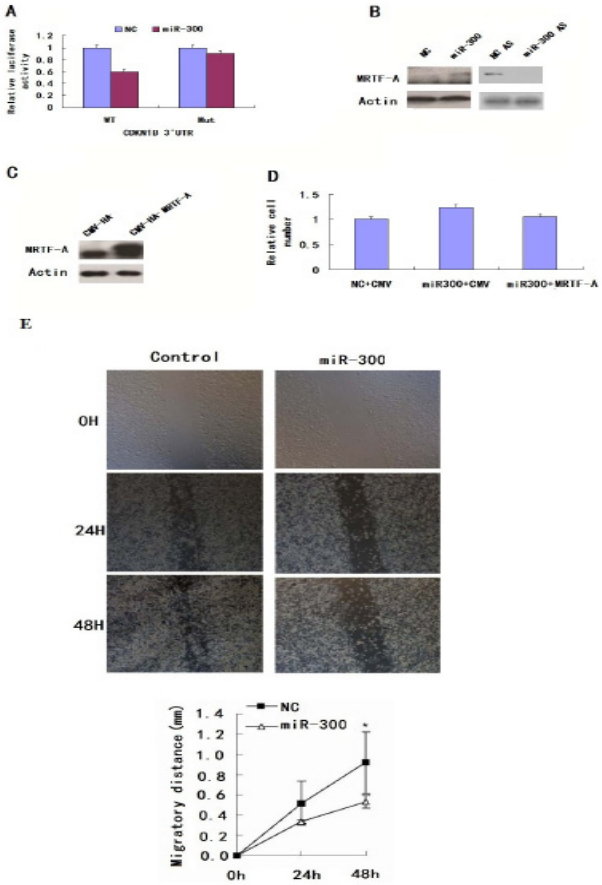

Figure 5. MRTF-A was a direct target of miR-300. (A) Luciferase activities were measured in cells co-transfected with the reporter constructs containing 3'UTR of MRTF-A with or without mutant and miR-300 mimic or negative-control miRNA. (B) Western blot assays showing the effect of miR300 on MRTF-A expression. (C) MRTF-A expression was significantly increased in MRTF-A transfected cells (CMV-HA-MRTF-A) compared with that in control cells (CMV-HA). (D) The numbers of viable cells were determined by cell count 72 hours after co-transfection with miR-300 mimic and CMV-HA-MRTF-A vector. (E) Wound healing experiment, the migration distance of VSMCs transfected with or without miR300. Values represent mean±SD. n=3. **p<0.01

was significantly up-regulated in atherosclerotic aortas, compared to normal aortas (Figure 3A). Consistent with that finding, cells positively stained for MRTF-A were observed within atherosclerotic lesions in the proximal aorta of ApoE$^{-/-}$ mice (Figure 3B). RT-PCR analysis showned that the expression of AQP1 in atherosclerotic aorta had no significant difference between Mkl1$^{-/-}$; ApoE$^{-/-}$ mice and Mkl1$^{+/+}$; ApoE$^{-/-}$ mice (Figure 3C). En-face analysis of the global progression of atherosclerotic lesions throughout the aorta revealed that the aortas of Mkl1$^{-/-}$; ApoE$^{-/-}$ mice contained smaller atherosclerotic lesions than those of Mkl1$^{+/+}$; ApoE$^{-/-}$ mice (Figure 3D). Furthermore, cross sectional analysis of the proximal aorta revealed the average lesion area at the aortic root of Mkl1$^{-/-}$; ApoE$^{-/-}$ mice (2.5%) to be significantly smaller than at the aortic root of Mkl1$^{+/+}$; ApoE$^{-/-}$ mice (11.8%, p<0.05 versus Mkl1$^{-/-}$; ApoE$^{-/-}$) (Figure 3E). Besides, we also found the moving ability of Mkl1$^{-/-}$; ApoE$^{-/-}$ mice to be significantly slowerly than at the aortic root of Mkl1$^{+/+}$; ApoE$^{-/-}$ mice (p<0.05 versus Mkl1$^{-/-}$; ApoE$^{-/-}$) (Figure 3F).

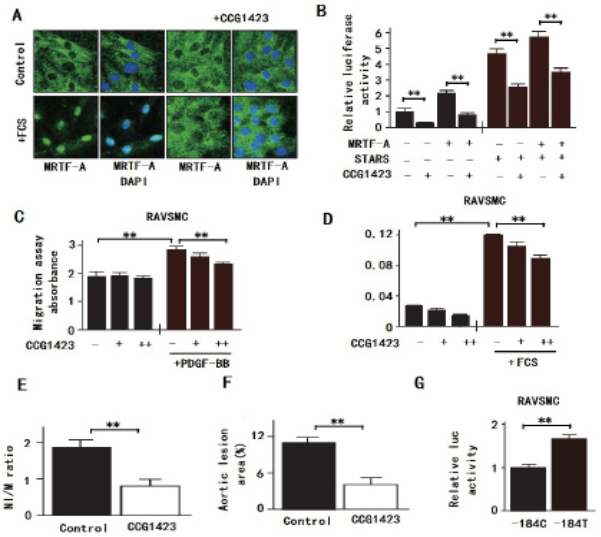

Figure 6. CCG-1423, an MRTF-A inhibitor, attenuated neointima formation induced by wire injury in mouse femoral arteries. (A) CCG-1423 diminished the nuclear accumulation of endogenous MRTF-A induced by 20% FCS in RAVSMCs. Cells were stained with anti-MRTF-A antibody (green) and DAPI (blue). (B) CCG-1423 significantly inhibited MRTF-A-induced SRF activity in RAVSMCs. Graphs show the relative luciferase activities of 3×CArG-luc. STARS: expression plasmid encoding striated muscle activator of Rho signaling. Data were obtained from two experiments performed in quintuplicate. (C) PDGF-BB-induced migration was assessed in RAVSMCs treated without or with 0.1 mm (+) or 1 mm (++) of CCG-1423. Data were obtained from two experiments performed in sex tuplicate. (D) FCS-induced migration was assessed in RAVSMCs treated without or with 0.1 mm (+) or 1mm (++) of CCG-1423. Data were obtained from two experiments performed in quadruplicate. (E) Effect of CCG-1423 on neointima formation in wire-injured femoral arteries in mice. Graph showing the neointima (NI)-tomedia (M) ratio in wire-injured arteries from mice treated without (control) or with CCG-1423 (n=3 in control group and 4 in CCG1423 group). (F) Graphs showing the relative (%) area of atherosclerotic lesions in cross-sections of proximal aorta from ApoE-/- mice fed a high cholesterol diet and treated with or without CCG-1423 for 6 weeks (n=3 in control group and 4 in CCG-1423 group). **p<0.01. (G) Effect of an SNP in the promoter region of MRTF-A gene (-184C>T) on the promoter activity in RAVSMCs. Relative activities of -930 bp MRTFA(-184C)-luc and -930 bp MRTF-A(-184T)-luc in two different experiments performed in quadruplicate are shown. All graphs are shown as means±s.e.m. **p<0.01

MRTF-A is necessary for acquisition of migratory capacity in dedifferentiated VSMCs

SRF controls cellular migration capacity in various cell types, including dedifferentiated VSMCs by regulating the expression of several target genes, including the genes encoding ICAM-1, MMP9 and integrin β1 (Du et al., 2009; Wang et al., 2013; Weinl et al., 2013). We therefore examined the expression of these SRF-target genes in wire-injured femoral arteries. We found that 2 weeks after wire injury there was significantly less expression of ICAM-1, MMP9 and integrin β1 genes in the injured femoral arteries of Mkl1$^{-/-}$ mice than control Mkl1$^{+/+}$ mice (Figure 4A). The levels of ICAM-1, MMP9, integrin β1 and AQP1 were significantly reduced after interfering with MRTF-A (Figure 4B). Over-expression of MRTF-A stimulated ICAM-1 promoter activity in an SRF-dependent manner in both primary rat aortic VSMCs (RAVSMCs) and NIH3T3 fibroblasts (Figure 4C), whereas interfering with MRTF-A reduced ICAM-1 promoter activity in RAVSMCs (Figure 4D). This supports the conclusion that MRTF-A regulates the expression of SRF-target genes in dedifferentiated VSMCs. Furthermore, interfering with MRTF-A significantly impaired PDGF-BB-induced RAVSMC migration (Figure 4E). Because SRF is also known to control cellular migration, we examined the effect of MRTF-A interference on RAVSMC migration, and found that interfering with MRTF-A significantly reduced serum-induced RAVSMC migration (Figure 4F).

MRTF-A was a direct target of miR-300

Luciferase reporter gene assay of miR-300 3' UTR wild type and mutant showed that in 3' UTR wild type, miR300 decreased the luciferase activity of MRTF-A, but in 3 ' UTR mutant, miR300 had no influence, which indicated that miR300 can reduce the expression of MRTF-A (Figure 5A). Western blot assays confirmed that MRTF-A expression were down-regulated by miR-300 (Figure 5B). MRTF-A expression was significantly increased in MRTF-A -transfected cells (CMV-HA-MRTF-A) compared with that in control cells (CMV-HA) (Figure 5C). The numbers of viable cells determined by cell count 72 hours after co-transfection with miR-300 and CMV-HA- MRTF-A vector didn't show significant difference (Figure 5D). In wound healing experiment, the migration distance of VSMCs transfected with miR300 was shorter than that without miR300 (Figure 5E).

Pharmacological inhibition of MRTF-A activity attenuates adverse vascular remodelling after wire injury

The results presented raise the possibility that MRTF-A is a novel therapeutic target for the treatment of vascular disease. Recently, a small molecule (CCG-1423) was found to inhibit Rho pathway-mediated SRF activation. CCG-1423 appears to inhibit the interaction between SRF and MRTF-A at a point upstream of the DNA binding.

Although the site of inhibition and its selectivity is not yet precisely defined, it was recently shown that CCG-1423 blocks nuclear translocation of MRTF-A, thereby inhibiting MRTF-A-mediated effects on SRF transcription, at least in part (Hanna et al., 2009; Jin et al., 2010). In addition, we confirmed that CCG-1423 blocks serum-induced nuclear accumulation of endogenous MRTF-A in RAVSMCs (Figure 6A). CCG-1423 also significantly blocked SRF activity induced by co-expression of striated muscle activator of rho signaling (STARS) and MRTF-A in RAVSMCs (Figure 6B). STARS is an actin-binding protein that activates SRF by inducing nuclear accumulation of MRTF-A. Both CCG-1423 and MRTF-A knockdown similarly inhibited STARS-induced activation of SRF in RAVSMCs. Similarly to knocking down MRTF-A, CCG-1423 significantly reduced the migration capacities of RAVSMCs (Figure 6C and D). When we then treated mice subjected to femoral artery wire injury with CCG-1423 (0.15 mg/kg intraperitoneally for 3 weeks), we found that CCG-1423 significantly attenuated the progression of vascular remodeling in arteries 3 weeks after injury (Figure 6E). Furthermore, as shown by Figure 6F, the relative (%) area of atherosclerotic lesions in cross-sections of proximal aorta from $ApoE^{-/-}$ mice fed a high cholesterol diet that treated with CCG-1423 for 6 weeks was significantly decreased (Figure 6F). After determined the effect of an SNP in the promoter region of MRTF-A gene (-184C>T) on the promoter activity in RAVSMCs, we found that the relative activitie of -930 bp MRTFA(-184C)-luc were significantly lower than that of -930 bp MRTF-A(-184T)-luc (Figure 6G).

Discussion

Angiogenesis is an important physiological process in which new blood vessels are generated by sprouting of existing ones. Dysregulated angiogenesis is implicated in many human diseases, including cancer and retinopathies (Du et al., 2009; Hanna et al., 2009). During angiogenesis, endothelial tip cells at the angiogenic front form numerous filopodia and guide vascularization, whereas stalk cells located behind tip cells are involved in proliferation and vessel extension (Lockman et al., 2007).

In the present study, we used two vascular injury models (femoral artery wire injury and diet induced atherosclerosis in $APOE^{-/-}$ mice) in $Mkl1^{-/-}$ mice to elucidate the roles played by MRTF-A in pathological vascular remodeling. We initially found that expression of MRTF-A and AQP1 were significantly increased in injured arteries and aortic tissues containing atherosclerotic lesions in $ApoE^{-/-}$ mice. In each model, neointima formation or atherosclerotic lesions were significantly smaller in $Mkl1^{-/-}$ mice than in the respective controls. The expression of ICAM-1, MMP-9, integrin β1 genes and AQP1, which are key regulators of cellular migration, was significantly diminished in the injured arteries of $Mkl1^{-/-}$ mice. However, AQP1 can promote tumour angiogenesis by allowing faster endothelial cell migration and sustaining an active endothelium (Nicchia GP et al.,2013). Knocking down MRTF-A in RAVSMCs reduced expression of these genes in response to extracellular stimuli, which significantly impaired cell migration. Recent studies revealed that we can repress the progression and metastasis of cancer cell via MRTF-A/B,which can activate the transcription of several actin cytoskeletal/focal adhesion genes SRF dependently to enhance the formation of stress fibers and focal adhesions (Yoshio T et al.,2010) . These results demonstrate that induced expression of MRTF-A is crucial for acquisition of the capacity to migrate in response to environmental stress in dedifferentiated VSMCs. We also found that MRTF-A gene expression in VSMCs is, at least in part, regulated by miR-300 (Lagna et al., 2007; Parmacek et al., 2007). Finally, we showed that a small molecule inhibitor of MRTF-A, CCG-1423, significantly reduced neointima formation following wire injury to mouse femoral arteries. Collectively, these results demonstrate that induction of MRTF-A plays a key role in vascular remodeling by maintaining SRF activity, thereby conferring a capacity for migration in response to extracellular stimuli on dedifferentiated VSMCs. MRTF-A is thus a potentially useful therapeutic target that may be more specific and efficient than the upstream Rho family GTPases, which can affect diverse intracellular signaling events.

The ability of MRTF-B to transduce Rho signaling into the nucleus is much weaker than that of MRTF-A (Staus et al., 2007; Hanna et al., 2009) so that Rho family signaling is almost exclusively confined to regulating contraction through modifying Ca^{2+} sensitivity in the cytosol (Hinson et al., 2007). Because MRTF-A is shuttled between the cytosol and nucleus (Lockman et al., 2004), where it activates SRF downstream of Rho family GTPase-actin signaling, in dedifferentiated VSMCs extracellular stimuli activating Rho GTPase signaling can substantively affect cellular proliferation and migration by modulating SRF activity (Smith et al., 2014; Dbouk et al., 2014). Loss or inhibition of MRTF-A reduced stimulus-induced cell migration, making cells static (Mah et al., 2014; Kanavi et al., 2014). This suggests that the expression of MRTF-A regulated by miR-300 regulates the plasticity of effectors downstream of Rho family signaling, thereby contributing to phenotypic modulation of VSMC during vascular remodeling.

In addition to the classical concept that dedifferentiated intimal VSMCs are derived from medial VSMCs, recent evidence raises the possibility that VSMC progenitor cells in the circulation or adventitia also contribute to intimal VSMCs (Bizenjima et al., 2014; da Cunha Morales Álvares et al., 2014). We have not addressed the role of MRTF-A in the process of intimal VSMC differentiation from such progenitor cells in this study. In that context, however, MRTF-A has been shown to be involved in the differentiation of mesenchymal stem cells into VSMCs (Mah et al., 2014). Thus, MRTF-A may also play an important role in the molecular processes underlying migration, proliferation and differentiation of VSMC progenitor cells into intimal VSMCs during vascular remodeling.

Recently, human genetic screening to identify novel susceptibility loci for CAD using micro-satellite markers and SNP analysis revealed that an SNP in the promoter region of the MRTF-A gene (-184C>T) is associated

with susceptibility to CAD (Garcia et al., 2014; Buckinx et al., 2014). Moreover, functional analysis suggested that heightened MRTF-A expression is associated with increased susceptibility to CAD (Maki et al., 2014; Moris et al., 2014). We observed that the MRTF-A promoter containing -184T, which is associated with high CAD susceptibility, showed significantly stronger transcriptional activity than the wild-type promoter in cultured VSMCs. These observations further support the conclusion that MRTF-A is crucially involved in pathological vascular remodeling underlying the development of vascular diseases (Mooren et al., 2014; Yoshida et al., 2014), and imply that MRTF-A is a potentially useful therapeutic target for prevention of the progression of vascular diseases.

Generally speaking, inhibition of MRTF-A expression is key to pathological remodeling underlying vascular disorders, as it sustains the SRF activity necessary for dedifferentiated VSMCs to acquire the capacity to migrate in response to extracellular stimuli. Our findings suggest that the expression of MRTF-A is mediated, at least in part, by microRNA (miR)-300 and contributes to the phenotypic modulation of VSMCs during vascular remodeling. These results point to MRTF-A as a potentially useful therapeutic target for the treatment of vascular diseases.

Acknowledgements

This research is supported by the National Natural Science Fundation of China (Grant No. 31100566), Chunmiao Cultivation Program for University Talents in Jilin Province (2013-352), Youth Research Fund Project of Science and Technology Department of Jilin Province (20140520006JH), the Training Program for Outstanding Young Talents in Jilin, Jilin Provincial Health Department Project (Grant No. 2011ZC029) .

References

Buckinx R, Bagyanszki M, Avula LR, et al (2014). Expression of corticotropin-releasing factor and urocortins in the normal and Schistosoma mansoni-infected mouse ileum. *Cell Tissue Res*, Epub ahead of print.

Bizenjima T, Seshima F, Ishizuka Y, et al (2014). Fibroblast growth factor-2 promotes healing of surgically created periodontal defects in streptozotocin-induced early diabetic rats via increasing cell proliferation and regulating angiogenesis. *J Clin Periodontol*, Epub ahead of print

Davis-Dusenbery BN, Chan MC, Reno KE, et al (2011). Down-regulation of Kruppel-like factor-4 (KLF4) by microRNA-143/145 is critical for modulation of vascular smooth muscle cell phenotype by transforming growth factor-beta and bone morphogenetic protein 4. *J Biol Chem*, **286**, 28097-110.

Du H, Wang X, Wu J, Qian Q (2009). Phenylephrine induces elevated RhoA activation and smooth muscle alpha-actin expression in Pkd2$^{+/-}$ vascular smooth muscle cells. *Hypertens Res*, **33**, 37-42.

Dbouk HA, Weil LM, Perera GK, et al (2014). Actions of the protein kinase WNK1 on endothelial cells are differentially mediated by its substrate kinases OSR1 and SPAK. *Proc Natl Acad Sci U S A*, Epub ahead of print.

da Cunha Morales Alvares A, Schwartz EF, Amaral NO, et al (2014). Bowman-birk protease inhibitor from vigna unguiculata seeds enhances the action of bradykinin-related peptides. *Molecules*, **19**, 17536-58.

Esteva-Font C1, Jin BJ, Verkman AS (2014). Aquaporin-1 gene deletion reduces breast tumor growth and lung metastasis in tumor-producing MMTV-PyVT mice. *Faseb J*, **28**, 1446-53.

Franco CA, Blanc J, Parlakian A, et al(2013). SRF selectively controls tip cell invasive behavior in angiogenesis. *Development*, **140**, 2321-33.

Garcia RA, Yan M, Search D, et al (2014). P2Y6 receptor potentiates pro-inflammatory responses in macrophages and exhibits differential roles in atherosclerotic lesion development. *PLoS One*, **9**, 111385.

Hanna M, Liu H, Amir J, et al (2009). Mechanical regulation of the proangiogenic factor CCN1/CYR61 gene requires the combined activities of MRTF-A and CREB-binding protein histone acetyltransferase. *J Biol Chem*, **284**, 23125-36.

Hinson JS, Medlin MD, Lockman K, Taylor JM, Mack CP (2007). Smooth muscle cell-specific transcription is regulated by nuclear localization of the myocardin-related transcription factors. *Am J Physiol Heart Circ Physiol*, **292**, 70-80.

Jeon ES, Heo SC, Lee IH, et al (2010). Ovarian cancer-derived lysophosphatidic acid stimulates secretion of VEGF and stromal cell-derived factor-1 alpha from human mesenchymal stem cells. *Exp Mol Med*, **42**, 280-93.

Jin L, Gan Q, Zieba BJ, et al (2010). The actin associated protein palladin is important for the early smooth muscle cell differentiation. *PLoS One*, **5**, 12823.

Kanavi MR, Darjatmoko S, Wang S, et al (2014). The sustained delivery of resveratrol or a defined grape powder inhibits newblood vessel formation in a mouse model of choroidal neovascularization. *Molecules*, **19**, 17578-603.

Lockman K, Taylor JM, Mack CP (2007). The histone demethylase, Jmjd1a, interacts with the myocardin factors to regulate SMC differentiation marker gene expression. *Circ Res*, **101**, 115-23.

Lagna G, Ku MM, Nguyen PH, et al (2007). Control of phenotypic plasticity of smooth muscle cells by bone morphogenetic protein signaling through the myocardin-related transcription factors. *J Biol Chem*, **282**, 37244-55.

Lockman K, Hinson JS, Medlin MD, et al (2004). Sphingosine 1-phosphate stimulates smooth muscle cell differentiation and proliferation by activating separate serum response factor co-factors. *J Biol Chem*, **279**, 42422-30.

Luo XG, Zhang CL, Zhao WW, et al (2013). Histone methyltransferase SMYD3 promotes MRTF-A-mediated transactivation of MYL9 and migration of MCF-7 breast cancer cells. *Cancer Lett*, **344**, 129-37.

Mah E, Pei R, Guo Y, et al (2014). Greater γ-tocopherol status during acute smoking abstinence with nicotine replacement therapy improved vascular endothelial function by decreasing 8-iso-15(S)-prostaglandin F2α. *Exp Biol Med*, Epub ahead of print.

Maki T, Okamoto Y, Carare RO, et al (2014). Phosphodiesterase III inhibitor promotes drainage of cerebrovascular β-amyloid. *Ann Clin Transl Neurol*, **1**, 519-33.

Moris DN, Kontos MI, Mantonakis EI, et al (2014). Concept of the aortic aneurysm repair-related surgical stress: a review of the literature. *Int J Clin Exp Med*, **7**, 2402-12.

Mooren OL, Li J, Nawas J, Cooper JA (2014). Endothelial cells use dynamic actin to facilitate lymphocyte transendothelial migration and maintain the monolayer barrier. *Mol Biol Cell*, Epub ahead of print.

Minami T, Kuwahara K, Nakagawa Y, et al (2012). Reciprocal expression of MRTF-A and myocardin is crucial for

pathologicalvascular remodelling in mice. *EMBO J*, **31**, 4428-40.

Mobasheri A, Barrett-Jolley R (2014). Aquaporin water channels in the mammary gland: from physiology to pathophysiology and neoplasia. *J Mammary Gland Biol*. **19**, 91-102.

Nakamura S, Hayashi K, Iwasaki K, et al (2010). Nuclear import mechanism for myocardin family members and their correlation withvascular smooth muscle cell phenotype. *J Biol Chem*, **285**, 37314-23.

Ni J, Dong Z, Han W, Kondrikov D, Su Y (2013). The role of RhoA and cytoskeleton in myofibroblast transformation in hyperoxic lung fibrosis. *Free Radic Biol Med*, **61**, 26-39.

Nicchia GP, Stigliano C, Sparaneo A, et al (2013). Inhibition of aquaporin-1 dependent angiogenesis impairs tumour growth in a mouse model of melanoma. *J Mol Med*, **91**, 613-23.

Parmacek MS (2007). Myocardin-related transcription factors: critical coactivators regulating cardiovascular development and adaptation. *Circ Res*, **100**, 633-44.

Shen D, Li J, Lepore JJ, et al (2011). Aortic aneurysm generation in mice with targeted deletion of integrin-linked kinase invascular smooth muscle cells. *Circ Res*, **109**, 616-28.

Staus DP, Blaker AL, Taylor JM, Mack CP (2007). Diaphanous 1 and 2 regulate smooth muscle cell differentiation by activating the myocardin-related transcription factors. *Arterioscler Thromb Vasc Biol*, **27**, 478-86.

Smith K, MacLeod D, Willie C, et al (2014). Influence of high altitude on cerebral blood flow and fuel utilization during exercise and recovery. *J Physiol*, Epub ahead of print.

Weinl C, Wasylyk C, Garcia Garrido M, et al (2014). Elk3 deficiency causes transient impairment in post-natal retinal vasculardevelopment and formation of tortuous arteries in adult murine retinae. *PLoS One*, **9**, 107048.

Wang D, Prakash J, Nguyen P, et al (2012). Bone morphogenetic protein signaling in vascular disease: anti-inflammatory action through myocardin-related transcription factor A. *J Biol Chem*, **287**, 28067-77.

Wang N, Zhang R, Wang SJ, et al (2013). Vascular endothelial growth factor stimulates endothelial differentiation from mesenchymal stem cells via Rho/myocardin-related transcription factor--a signaling pathway. *Int J Biochem Cell Biol*, **45**, 1447-56.

Weinl C, Riehle H, Park D, et al (2013). Endothelial SRF/MRTF ablation causes vascular disease phenotypes in murine retinae. *J Clin Invest*, **123**, 2193-206.

Yoshida S, Kobayashi Y, Nakama T, et al (2014). Increased expression of M-CSF and IL-13 in vitreous of patients with proliferative diabetic retinopathy: implications for M2 macrophage-involving fibrovascular membrane formation. Br J Ophthalmol, Epub ahead of print.

Yoshio T, Morita T, Tsujii M, et al (2010). MRTF-A/B suppress the oncogenic properties of v-ras- and v-src-mediated transformants. *Carcinogenesis*, **31**, 1185-93.

Zhang C, Luo X, Liu L, et al (2013). Myocardin-related transcription factor A is up-regulated by 17β-estradiol and promotes migration of MCF-7 breast cancer cells via transactivation of MYL9 and CYR61. *Acta Bioch Bioph Sin*, **45**, 921-7.